


ORIGINAL RESEARCH

Open Access



Biodistribution and radiation dosimetry of the novel hypoxia PET probe [¹⁸F]DiFA and comparison with [¹⁸F]FMISO

Shiro Watanabe¹, Tohru Shiga^{1*} , Kenji Hirata¹, Keiichi Magota², Shozo Okamoto^{1,3}, Takuya Toyonaga¹, Kei Higashikawa⁴, Hironobu Yasui⁴, Jun Kobayashi⁵, Ken-ichi Nishijima^{4,6}, Ken Iseki^{5,7}, Hiroki Matsumoto⁸, Yuji Kuge^{1,4} and Nagara Tamaki^{1,9}

Abstract

Background: To facilitate hypoxia imaging in a clinical setting, we developed 1-(2,2-dihydroxymethyl-3-[¹⁸F]-fluoropropyl)-2-nitroimidazole ([¹⁸F]DiFA) as a new tracer that targets tumor hypoxia with its lower lipophilicity and efficient radiosynthesis. Here, we evaluated the radiation dosage, biodistribution, human safety, tolerability, and early elimination after the injection of [¹⁸F]DiFA in healthy subjects, and we performed a preliminary clinical study of patients with malignant tumors in a comparison with [¹⁸F]fluoromisonidazole ([¹⁸F]FMISO).

Results: The single administration of [¹⁸F]DiFA in 8 healthy male adults caused neither adverse events nor abnormal clinical findings. Dynamic and sequential whole-body scans showed that [¹⁸F]DiFA was rapidly cleared from all of the organs via the hepatobiliary and urinary systems. The whole-body mean effective dose of [¹⁸F]DiFA estimated by using the medical internal radiation dose (MIRD) schema with organ level internal dose assessment/exponential modeling (OLINDA/EXM) computer software 1.1 was $14.4 \pm 0.7 \mu\text{Sv/MBq}$. Among the organs, the urinary bladder received the largest absorbed dose ($94.7 \pm 13.6 \mu\text{Sv/MBq}$). The mean absorbed doses of the other organs were equal to or less than those from other hypoxia tracers. The excretion of radioactivity via the urinary system was very rapid, reaching $86.4 \pm 7.1\%$ of the administered dose. For the preliminary clinical study, seven patients were subjected to [¹⁸F]FMISO and [¹⁸F]DiFA positron emission tomography (PET) at 48-h intervals to compare the two tracers' diagnostic ability for tumor hypoxia. The results of the tumor hypoxia evaluation by [¹⁸F]DiFA PET at 1 h and 2 h were not significantly different from those obtained with [¹⁸F]FMISO PET at 4 h ([¹⁸F]DiFA at 1 h, $p = 0.32$; [¹⁸F]DiFA at 2 h, $p = 0.08$). Moreover, [¹⁸F]DiFA PET at both 1 h ($k = 0.68$) and 2 h ($k = 1.00$) showed better inter-observer reproducibility than [¹⁸F]FMISO PET at 4 h ($k = 0.59$).

Conclusion: [¹⁸F]DiFA is well tolerated, and its radiation dose is comparable to those of other hypoxia tracers. [¹⁸F]DiFA is very rapidly cleared via the urinary system. [¹⁸F]DiFA PET generated comparable images to [¹⁸F]FMISO PET in hypoxia imaging with shorter waiting time, demonstrating the promising potential of [¹⁸F]DiFA PET for hypoxia imaging and for a multicenter trial.

Keywords: Hypoxia, PET, New tracer, Dosimetry

* Correspondence: tshiga@med.hokudai.ac.jp

¹Department of Nuclear Medicine, Graduate School of Medicine, Hokkaido University, Kita-15, Nishi-7, Kita-ku, Sapporo 060-8638, Japan
Full list of author information is available at the end of the article

Background

There is accumulating evidence that tumor hypoxia induces the expression of gene products that confer tumor propagation, malignant progression, and broad resistance to therapy [1]. Positron emission tomography (PET) is a useful clinical tool to visualize hypoxia in vivo. Among hypoxia PET tracers, [^{18}F]fluoromisonidazole ([^{18}F]FMISO) is the most extensively studied; however, its optimal acquisition time is 3–4 h after injection due to its slow specific accumulation in hypoxic tissue as well as its slow clearance from the plasma [2, 3]. Consequently, next-generation tracers such as [^{18}F]fluoroazomycinarabinofuranoside ([^{18}F]FAZA), [^{18}F]fluoroerythronitromidazole ([^{18}F]FET-NIM), and [^{18}F]-3-fluoro-2-(4-((2-nitro-1H-imidazol-1-yl)methyl)-1H-1,2,3-triazol-1-yl)propan-1-ol ([^{18}F]HX4) have been developed and applied to clinical trials [4]. Like [^{18}F]FMISO, these hypoxia probes are derived from the 2-nitroimidazole in their structures. However, they still have the clinical drawbacks of poor imaging contrast at acquisition time and limited reproducibility [5, 6].

We recently developed a new imaging tracer targeting tumor hypoxia, 1-(2,2-dihydroxymethyl-3-[^{18}F]-fluoropropyl)-2-nitroimidazole ([^{18}F]DiFA), to overcome the disadvantages of [^{18}F]FMISO and obtain better contrast image quality in a shorter period of time. [^{18}F]DiFA has lower lipophilicity and is thus expected to be excreted more rapidly via the urinary system. Moreover, as another advantage, we aimed to avoid enantiomers in the structure of [^{18}F]DiFA to ensure efficient synthesis and quality control, which should make hypoxia imaging more readily available for clinical application. Shimizu et al. elucidated that the mechanism by which [^{18}F]DiFA and [^{18}F]FMISO targets hypoxia is the same [7].

In the present study, we first evaluated the radiation dosage, biodistribution, human safety, tolerability, and early elimination of ^{18}F activity in urine after the injection of a single dose of [^{18}F]DiFA in healthy volunteers. We then, for the first time, compared the hypoxia detectability of [^{18}F]DiFA and [^{18}F]FMISO in patients with malignant tumors.

Subjects and methods

Healthy volunteers and patients

Eight healthy male adults (ages 21–39 years, weight 55.1–74.1 kg, Table 1) who passed the screening tests were recruited for the first-in-human study, and seven patients (ages 48–68 years, four men and three women, Table 2) were recruited for the preliminary study of [^{18}F]DiFA. All seven patients had histopathologically confirmed malignant tumors which were identified in the prior imaging test.

Radiopharmaceutical preparation

[^{18}F]DiFA was prepared by the nucleophilic fluorination of 2,2-dimethyl-5-[2-(2-nitro-1H-imidazole-1-yl)ethyl]-5-

Table 1 Male volunteer-specific data

No.	Age	Weight (kg)	Dose (MBq)	Mass (μg)
1	25	66.4	182.6	0.088
2	37	55.1	353.3	0.209
3	22	74.1	718.7	0.361
4	27	60.0	727.0	0.481
5	22	57.4	729.7	0.336
6	27	55.1	692.6	0.357
7	24	69.7	724.2	0.312
8	22	55.9	722.0	0.337
Mean	25.8 \pm 4.7	61.7 \pm 6.0	606.3 \pm 200.2	0.310 \pm 0.109

(p-toluenesulfonyloxymethyl)-1,3-dioxane followed by acidic hydrolysis of the protecting group using an automated synthesis apparatus (UG-M1; Universal Giken, Odawara, Japan) (Fig. 1, Additional file 1: Table S1).

[^{18}F]FMISO was prepared by the nucleophilic fluorination of the precursor molecule 1-(2'-nitro-1'-imidazolyl)-2-O-tetrahydropyranyl-3-O-toluenesulphonylpropanediol in a manner similar to that for [^{18}F]DiFA using previously reported procedures [8, 9].

The product specifications of radiochemical purity were set to be > 95% for [^{18}F]DiFA and [^{18}F]FMISO in accordance with the previous report on [^{18}F]FMISO [10]. The actual radiochemical purity used in the present study was 99.0 \pm 1.0% for [^{18}F]DiFA and > 95% for [^{18}F]FMISO.

Biodistribution, dosimetry, and safety of [^{18}F]DiFA in the healthy volunteers

The biodistribution and dosimetry procedure are shown in Fig. 2. [^{18}F]DiFA was intravenously injected over a 1-min period. We increased the injected activity in a step-by-step manner. Volunteers #1 and #2 were injected with 185 MBq and 370 MBq of [^{18}F]DiFA, respectively, following approval by a third-party safety committee. The other six volunteers (#3–#8) were injected with 740 MBq of [^{18}F]DiFA.

After the injection, the emission study was started with a 5-min dynamic scanning with the field of view (FOV) containing the entire heart, followed by serial three-bed scanning covering from the heart to the kidneys until 60 min post-injection, on a Gemini TF PET/computed tomography (CT) scanner (Philips Healthcare, Cleveland, OH). After the dynamic scanning, five serial whole-body PET scans were acquired at 1, 2, 4, 6, and 24 h post-injection. Prior to each emission imaging session, a whole-body low-dose CT image was acquired for attenuation and scatter corrections. The whole-body PET scans were acquired in 3D mode and ranged from the vertex to the toes. The duration of emission scanning was 1.5 min per bed position.

Table 2 Characteristics of the seven patients with malignant tumors

No.	Age	Sex	Weight (kg)	FMISO activity (MBq)	DiFA activity (MBq)	DiFA mass (μg)	Diagnosis
1	68	M	65	394.2	703.1	0.338	Undifferentiated pleomorphic sarcoma
2	64	F	61	384.7	714.5	0.236	Small cell lung cancer
3	56	M	60	385.6	715.6	0.237	Rectal adenocarcinoma
4	63	F	51	374.6	725.2	0.277	Tongue squamous cell carcinoma
5	64	M	73	386.5	716.9	0.274	Liposarcoma
6	65	M	76	387.4	716.4	0.299	Hepatocellular carcinoma
7	48	F	52	386.5	733.3	0.306	Malignant melanoma
Mean	61.1 \pm 6.3		62.6 \pm 8.9	385.6 \pm 5.4	717.9 \pm 8.7	0.281 \pm 0.034	

The PET images were reconstructed using 3-dimensional blob-based iterative list-mode ordered-subsets expectation maximization (OSEM) algorithm with time-of-flight information, following default settings: iterations, 3; subsets, 33; blob increment, 2.0375 voxels; blob radius, 2.5 voxels; blob shape parameter alpha, 8.3689; and relaxation parameter, 0.7. The image matrix size was 144×144 pixels for the 576-mm FOV, and the voxel size was $4 \times 4 \times 4 \text{ mm}^3$. The reconstruction included corrections for normalization, dead time, attenuation, scatter, random coincidences, sensitivity, and decay. The reconstructed images were not additional post-filtered.

PET images for volunteers #3–#8 were analyzed using PMOD software ver. 3.1 (PMOD Technologies, Zurich, Switzerland). The uptake of each major organ was calculated by drawing a volume of the region based on the contours of the PET and CT images as described previously [11]. At each time point, the decayed radioactivity of each source organ is expressed as a percentage of the injected activity (%IA) and plotted against time, and fitted to an exponential or sum-of-exponentials function in organ level internal dose assessment/exponential modeling (OLINDA/EXM) 1.1 computer software (Vanderbilt University, Nashville, TN) [12] to determine the total number of disintegrations per unit of administered activity, hereafter referred to as the normalized number of disintegrations.

Urine samples were collected for the following intervals: 0–1 h, 1–2 h, 2–4 h, 4–6 h, 6–9 h, and 9–24 h. The urine samples were assayed for radioactivity with an auto-well gamma counter (ARC-400; Hitachi, Tokyo) to estimate the total excreted activity. The residence time of the urinary bladder was also determined using the dynamic bladder model in OLINDA/EXM 1.1 as described previously [11].

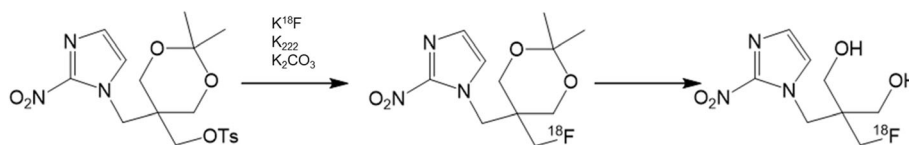
Voiding intervals were set to 2 h to calculate the dose estimates for the urinary bladder wall. The effective doses in the various organs were calculated by entering the normalized number of disintegrations of all source organs for each subject into OLINDA/EXM, using the standardized adult male models. Data are shown as the mean \pm standard deviation.

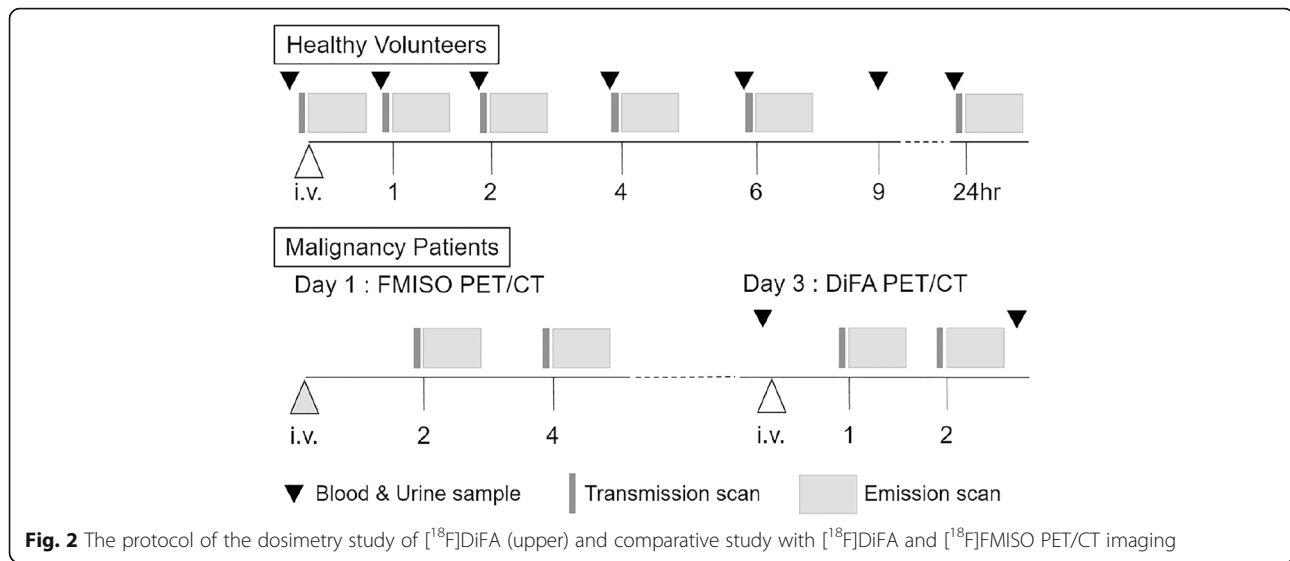
The subjects' blood pressure, body temperature, pulse rate, oxygen saturation, blood, and urine sampling were monitored before the administration of [^{18}F]DiFA and following all PET/CT scans in addition to 9 h after the administration of [^{18}F]DiFA.

Patient study

All seven patients underwent both [^{18}F]DiFA and [^{18}F]FMISO scans with a 2-day interval. All patients were injected with up to 740 MBq of [^{18}F]DiFA and 400 MBq of [^{18}F]FMISO. PET scans were acquired at 1 and 2 h post-injection, and [^{18}F]FMISO PET scans were acquired at 2 and 4 h post-injection. The reconstruction method was the same as that used with the whole-body PET scanning in this first-in-humans study, and the scanning of the lesion was performed for 10 min.

All PET/CT images were independently visually interpreted using XTREK software (J-MAC Systems, Sapporo, Japan) by two experienced certified specialists in nuclear medicine (SW and KH). The observers were blinded both to the tracer and to the timing of the scan. The observers used both gray and color scales where the upper and lower limits could be changed manually. The tracer uptake in the lesions over 10 mm in size was assessed and assigned an intensity uptake score of 0–4 as follows: 0, uptake less than background; 1, no regions of focal uptake

**Fig. 1** Synthesis of [^{18}F]DiFA from its precursor



greater than background; 2, focal uptake mildly greater than background; 3, focal uptake moderately greater than background; and 4, focal uptake markedly greater than background. The normal area of the same organ where the tumor existed, or normally-appearing muscle if the tumor existed in fatty tissues such as retroperitoneum, was chosen as the background. As the next step, the lesions were grouped into two classes: those with uptake scores of ≥ 2 were considered hypoxia-positive and the others were deemed hypoxia-negative.

Histopathological confirmation was not practical in all of the lesions. The lesions were considered positive when the 4-h [^{18}F]FMISO PET image was positive, based on the general consensus that [^{18}F]FMISO is the gold standard in clinical research for the measurement of hypoxia. Cases of disagreement were resolved by consensus.

The inter-observer agreement regarding the specialists' visual analysis and the hypoxia positivity of the lesions was evaluated using kappa values. The sensitivity, specificity, and accuracy of hypoxia were evaluated in the [^{18}F]DiFA PET.

The quality of the agreements was defined as follows, according to the Cohen k test: 0–0.2, poor agreement; 0.21–0.40, fair agreement; 0.41–0.60, moderate agreement; 0.61–0.80, good agreement; and 0.81–1.00, very good agreement. For each imaging protocol, diagnostic performances (sensitivity, specificity, and accuracy) were assessed and compared using the McNemar test. Statistical calculations were carried out using JMP[®] 14 software (SAS, Cary, NC, USA).

Results

Safety of [^{18}F]DiFA

None of the eight volunteers presented with any symptoms or clinically detectable adverse pharmacological

effects. No significant changes in vital signs or the results of laboratory tests were observed during the first 24-h observation period following the tracer administration or the follow-up visit at 1 week (Additional file 2). The radiation exposure of attenuation correction CT in volunteers was totally 43.0 ± 0.9 mSv.

Imaging and biodistribution of [^{18}F]DiFA

The main characteristics of the radiotracer uptake are illustrated in PET maximum intensity projection (MIP) images for one of the normal volunteers from the PET scans in Fig. 3. In the early scans, a predominant accumulation was observed in the subjects' urinary tract (the renal pelvis, ureter, and bladder) with moderate uptake in the liver. The gallbladder and large intestine showed strong radioactivity in later scans. The brain showed no significant uptake (even lower than muscles), reflecting the hydrophilic characteristics of [^{18}F]DiFA. All other organs showed background levels of activity.

In all eight subjects, the highest (decay-corrected) uptake of [^{18}F]DiFA was found in the muscle, with peak values of $26.2 \pm 3.4\%$ injected activity (IA), followed by the liver at $5.7 \pm 1.2\%$ IA. The %IA decreased gradually toward the end of the study in all organs except for the brain and gallbladder (Fig. 4). Although the radioactivity of [^{18}F]DiFA was excreted primarily via the renal system, a small portion of [^{18}F]DiFA was excreted via the bile system. By the end of the study (20–24 h), approx. $86.4 \pm 7.1\%$ of the injected activity of [^{18}F]DiFA had been excreted in the urine (Fig. 5). This clearance was relatively rapid among hypoxia tracers, with $20.2 \pm 1.6\%$ of the tracer being excreted by 1 h after the injection.

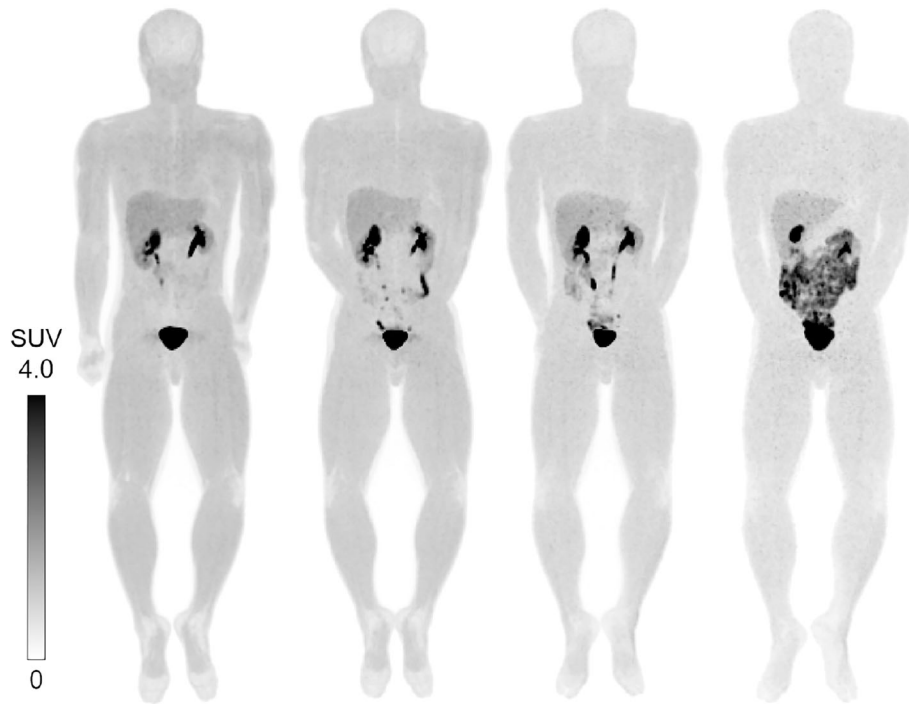


Fig. 3 MIP images of $[^{18}\text{F}]\text{DiFA}$ in a healthy volunteer. Decay-corrected anterior maximum-intensity projections of PET at 1, 2, 4, and 6 h (from left to right) after an injection of 718.7 MBq of $[^{18}\text{F}]\text{DiFA}$ in a 74.0-kg male volunteer. There was a rapid clearance of activity in the kidneys, liver, and bladder. Gallbladder activity peaked following the first meal after the PET acquisition at 4 h, then decreased with time

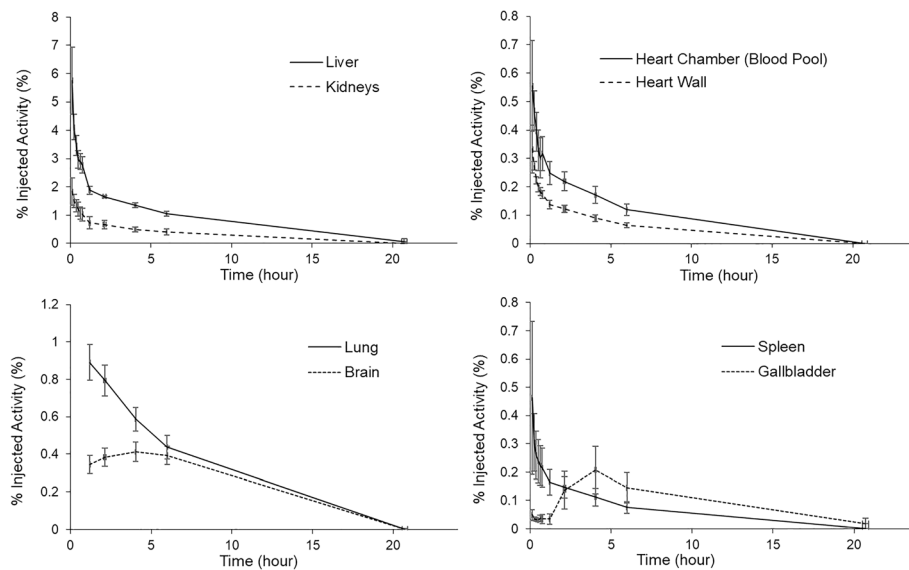


Fig. 4 Time-activity curves in representative organs. $[^{18}\text{F}]\text{DiFA}$ was rapidly cleared from the organs. The accumulation in the gallbladder peaked after 4 h, since $[^{18}\text{F}]\text{DiFA}$ that was excreted in the bile due to hepatobiliary excretion stayed in the gallbladder and was secreted with a meal (at 4 h after examination). The accumulation in the brain slowly increased, reflecting the improvement in water solubility, and after 4 h, it peaked and then decreased. The data are the mean \pm SD of results from six volunteers

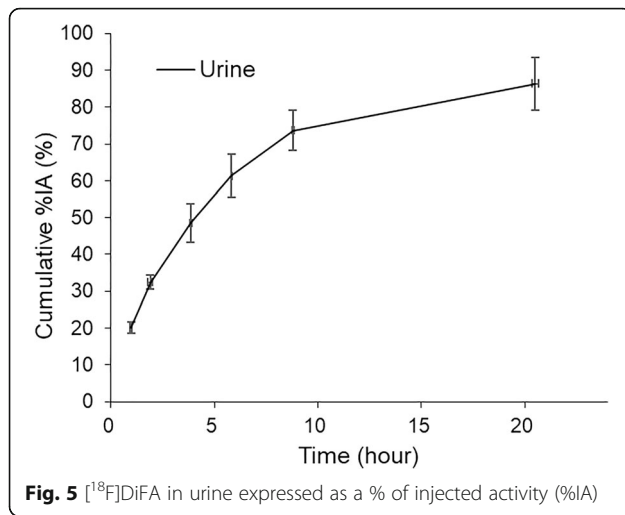


Fig. 5 $[^{18}\text{F}]\text{DiFA}$ in urine expressed as a % of injected activity (%IA)

Dosimetry of $[^{18}\text{F}]\text{DiFA}$

The mean residence times for the organs are listed in Table 3. The mean effective dose of $[^{18}\text{F}]\text{DiFA}$ was estimated as $14.4 \pm 0.7 \mu\text{Sv}/\text{MBq}$ for the 2-h bladder-voiding models. The highest radiation-equivalent dose was calculated for the urinary bladder wall, with $0.09 \text{ mSv}/\text{MBq}$ (Table 4).

Comparison of $[^{18}\text{F}]\text{DiFA}$ and $[^{18}\text{F}]\text{FMISO}$ in patients

The seven patients had 19 lesions that could be evaluated. The radiation exposure of attenuation correction CT and FMISO was $2.9 \pm 1.5 \text{ mSv}$ and $5.0 \pm 0.1 \text{ mSv}$, respectively.

The visual analyses of $[^{18}\text{F}]\text{DiFA}$ PET at both 1 h and 2 h compared to $[^{18}\text{F}]\text{FMISO}$ at 4 h are shown in Table 5.

Table 3 Residence times of $[^{18}\text{F}]\text{DiFA}$ for measured source organs

Brain	0.009 ± 0.001
Gallbladder contents	0.003 ± 0.001
Lower large intestine	0.002 ± 0.000
Small intestine	0.024 ± 0.004
Upper large intestine	0.013 ± 0.002
Heart contents	0.007 ± 0.001
Heart wall	0.004 ± 0.000
Kidneys	0.021 ± 0.004
Liver	0.057 ± 0.004
Lungs	0.020 ± 0.002
Muscle	0.542 ± 0.052
Pancreas	0.003 ± 0.001
Red marrow	0.098 ± 0.013
Spleen	0.005 ± 0.002
Remainder	1.066 ± 0.104
Urinary bladder contents (2 h)	0.184 ± 0.027

The data are mean \pm SD (hour), $n = 6$ patients

Table 6 shows the global agreements of the visual analyses of $[^{18}\text{F}]\text{FMISO}$ and $[^{18}\text{F}]\text{DiFA}$ PET/CT images. The inter-observer agreement of the five-level grading was better for $[^{18}\text{F}]\text{DiFA}$ ($\kappa = 0.60$ at 1 h, 1.00 at 2 h) than for $[^{18}\text{F}]\text{FMISO}$ ($\kappa = 0.29$ at 2 h, 0.38 at 4 h) in this study.

The diagnostic performance $[^{18}\text{F}]\text{DiFA}$ is summarized in Table 7. There was no significant difference in the detection of tumor hypoxia between $[^{18}\text{F}]\text{FMISO}$ and $[^{18}\text{F}]\text{DiFA}$ (Fig. 6).

Discussion

In this work, we first evaluated the safety and dosimetric data of $[^{18}\text{F}]\text{DiFA}$, a new $[^{18}\text{F}]\text{FMISO}$ -based derivative with stronger hydrophilicity, in healthy volunteers for its potential use as a hypoxia PET tracer. We found that $[^{18}\text{F}]\text{DiFA}$ caused no adverse effects after injection and had rapid clearance from the urine and reasonable biodistribution and dosimetry profiles in human subjects. In addition, in our comparison of the abilities of $[^{18}\text{F}]\text{DiFA}$ and $[^{18}\text{F}]\text{FMISO}$ to diagnose tumor hypoxia, we found that the diagnostic abilities were approximately equivalent, and good inter-observer reproducibility was observed even though there was a shorter time from the injection to the scan with the use of $[^{18}\text{F}]\text{DiFA}$.

In our human study, high $[^{18}\text{F}]\text{DiFA}$ uptake/excretion was observed in the liver, muscle, and kidneys, whereas low uptake was observed in the lung and brain. These findings are similar to those for other hypoxia tracers, and the usefulness of evaluating neoplasms in the cranial should be investigated in detail. $[^{18}\text{F}]\text{DiFA}$ clearance from the blood pool is very rapid, and the accumulation in the blood pool was obscured at just 1 h after administration. In addition, since the distributions in the liver and intestines were relatively low, patients with hepatobiliary and colorectal cancers may be good candidates for hypoxia imaging using $[^{18}\text{F}]\text{DiFA}$ if the images are acquired at an appropriate time point.

$[^{18}\text{F}]\text{DiFA}$ had a higher rate of urinary excretion (86.4%) than other hypoxia tracers, such as $[^{18}\text{F}]\text{FAZA}$ (15% [11]), $[^{18}\text{F}]\text{FETNIM}$ (60% [15]), and $[^{18}\text{F}]\text{HX4}$ (45% at 3.6 h [14]). In general, more hydrophilic compounds will have more rapid biodistribution and clearance from the body [16]. $[^{18}\text{F}]\text{DiFA}$ may thus be the ideal tracer for hypoxia imaging. In a comparison of our present dosimetry data with the available literature on $[^{18}\text{F}]\text{FMISO}$ [13], $[^{18}\text{F}]\text{FAZA}$ [11], $[^{18}\text{F}]\text{HX4}$ [14], and $[^{18}\text{F}]\text{FETNIM}$ [15], radiation dose of these tracers resulted in almost the same distribution as that of $[^{18}\text{F}]\text{DiFA}$. Although, in the case of $[^{18}\text{F}]\text{DiFA}$, the radiation dose to the bladder wall is increased due to the high water solubility of this tracer, it is expected that the actual radiation dose can be reduced by shortening the urinary excretion interval (i.e., frequent voiding). No acute radiation toxicity was expected with 740 MBq F-18. Also, no chemical toxicity

Table 4 Equivalent doses of [¹⁸F]DiFA, [¹⁸F]FMISO, [¹⁸F]FAZA, [¹⁸F]HX4, and [¹⁸F]FETNIM to target organs

Target organs	Tracer				
	[¹⁸ F]DiFA (2-h void)	[¹⁸ F]FMISO [13] (2-h void)	[¹⁸ F]FAZA [11] (2-h void)	[¹⁸ F]HX4 [14] (1-h void)	[¹⁸ F]FETNIM [15] (2-h void)
Adrenals	0.009 ± 0.000	0.017	0.012 ± 0.001	0.009 ± 0.001	0.012
Brain	0.004 ± 0.000	0.009	0.004 ± 0.001	0.005 ± 0.001	0.006
Breasts	0.006 ± 0.000	0.012	0.009 ± 0.001	0.006 ± 0.001	0.007
Gallbladder wall	0.014 ± 0.002	0.015	0.013 ± 0.004	0.024 ± 0.007	0.014
LLI wall	0.013 ± 0.001	0.014	0.013 ± 0.006	0.022 ± 0.002	0.012
Small intestine	0.015 ± 0.001	0.013	0.012 ± 0.005	0.015 ± 0.000	0.012
Stomach wall	0.009 ± 0.000	0.013	0.012 ± 0.001	0.009 ± 0.001	0.012
ULI wall	0.015 ± 0.001	0.014	0.013 ± 0.002	0.016 ± 0.003	0.014
Heart wall	0.008 ± 0.000	0.019	0.018 ± 0.001	0.009 ± 0.001	0.011
Kidneys	0.018 ± 0.003	0.016	0.017 ± 0.002	0.019 ± 0.002	0.027
Liver	0.011 ± 0.001	0.018	0.016 ± 0.003	0.014 ± 0.003	0.024
Lungs	0.008 ± 0.000	0.010	0.011 ± 0.008	0.008 ± 0.001	0.008
Muscle	0.008 ± 0.000	0.014	0.011 ± 0.009	0.008 ± 0.001	0.012
Ovaries	0.012 ± 0.000	0.018	0.014 ± 0.001	0.012 ± 0.001	0.013
Pancreas	0.012 ± 0.002	0.018	0.013 ± 0.002	0.010 ± 0.001	0.019
Red marrow	0.014 ± 0.001	0.011	0.011 ± 0.001	0.008 ± 0.001	0.012
Osteogenic cells	0.014 ± 0.000	0.008	0.011 ± 0.002	0.012 ± 0.001	0.011
Skin	0.006 ± 0.000	0.005	0.008 ± 0.001	0.006 ± 0.001	0.007
Spleen	0.010 ± 0.002	0.016	0.017 ± 0.008	0.009 ± 0.001	0.020
Testes	0.009 ± 0.000	0.015	0.004 ± 0.001	0.009 ± 0.001	0.010
Thymus	0.007 ± 0.000	0.016	0.011 ± 0.003	0.008 ± 0.001	0.009
Thyroid	0.007 ± 0.000	0.015	0.010 ± 0.001	0.008 ± 0.001	0.009
Urinary bladder wall	0.095 ± 0.014	0.021	0.047 ± 0.008	0.085 ± 0.010	0.062
Uterus	0.015 ± 0.001	0.018	0.020 ± 0.001	0.014 ± 0.001	0.015
Total body	0.009 ± 0.000	0.013	0.012 ± 0.002	0.008 ± 0.001	0.011
Effective dose	0.014 ± 0.001	0.013	0.013 ± 0.004	0.014 ± 0.001	0.015

LLI lower large intestine, ULI upper large intestine. The data are mean ± SD/mean, mSv/MBq, n = 6 subjects.

was expected with the unlabeled part of the 0.310 ± 0.109 µg DiFA since the maximum non-toxic dose was 517 µg/kg based on our preclinical study. We confirmed that there was no toxicity based on the laboratory tests.

To assess the potential of [¹⁸F]DiFA as a specific PET tracer for hypoxia imaging, we examined seven patients with malignant tumors by both [¹⁸F]FMISO and [¹⁸F]DiFA PET/CT imaging. In this study, there was a 48-h interval between [¹⁸F]FMISO and [¹⁸F]DiFA imaging. Hypoxia is an unstable condition that can be altered in a short time, theoretically explained by acute and chronic hypoxia. In our

previous clinical study using [¹⁸F]FMISO, however, we confirmed that the degree and localization of hypoxia were stable between 2 scans of [¹⁸F]FMISO-PET with 48 h interval [17]. Therefore, we assumed that the hypoxia status was stable between [¹⁸F]FMISO and [¹⁸F]DiFA imaging. The results showed that there were no significant differences between [¹⁸F]FMISO and [¹⁸F]DiFA PET for the detection of tumor hypoxia. Moreover, [¹⁸F]DiFA PET at both 1 and 2 h post-injection showed better inter-observer reproducibility than [¹⁸F]FMISO at 4 h. Because [¹⁸F]FMISO has characteristics of slow accumulation and slow clearance

Table 5 Performance of [¹⁸F]DiFA in detecting hypoxia compared to [¹⁸F]FMISO at 4 h

	Observer 1		Observer 2		Observer 1 and 2	
	[¹⁸ F]DiFA (1 h (+))	[¹⁸ F]DiFA (1 h (-))	[¹⁸ F]DiFA (1 h (+))	[¹⁸ F]DiFA (1 h (-))	[¹⁸ F]DiFA (2 h (+))	[¹⁸ F]DiFA (2 h (-))
[¹⁸ F]FMISO at 4 h (+)	9	0	8	1	9	0
[¹⁸ F]FMISO at 4 h (-)	1	9	3	7	3	7

Table 6 κ value for PET/CT images

κ	$[^{18}\text{F}]\text{FMISO}$		$[^{18}\text{F}]\text{DiFA}$	
	2 h	4 h	1 h	2 h
Five classes	0.29	0.63	0.60	1.00
Two classes	0.38	0.59	0.68	1.00

from blood and normal tissues, background organs often show high accumulation when imaged, resulting in a low tumor-to-background ratio (Fig. 6). Early scans are greatly affected by perfusion and degrade accuracy and reproducibility. However, the image quality was poor in $[^{18}\text{F}]\text{FMISO}$ PET image 4 h after injection due to $> 2\times$ half-life of F-18. We think these are the main reasons for degraded inter-operator reproducibility for $[^{18}\text{F}]\text{FMISO}$ PET. In contrast, $[^{18}\text{F}]\text{DiFA}$ is rapidly cleared from the blood and normal tissues, enhancing lesion-to-background contrast. In addition, early scan timing keeps a high signal-to-noise ratio, which leads to good image quality. The rapid clearance of $[^{18}\text{F}]\text{DiFA}$ provided an easy evaluation and high reproducibility. From our results, 4 h $[^{18}\text{F}]\text{FMISO}$ PET has considered the reference standard in clinical and $[^{18}\text{F}]\text{DiFA}$ PET showed 3 false positives out of 10 lesions. The disparity between the two tracer datasets may be mainly due to the pharmacokinetics of the tracer itself, but also partly by the possible fluctuation of hypoxic status (so-called, acute hypoxia).

The tracer activity was determined by our preclinical study of dose exposure using rat. The activity of 740 MBq of $[^{18}\text{F}]\text{DiFA}$ was acceptable for the first-in-man study as maximum activity, and we confirmed its safety in healthy subjects and cancer patients. From this dataset, we will determine the optimal activity of $[^{18}\text{F}]\text{DiFA}$. Wang et al. [18] and Thorwarth et al. [19] reported that the kinetic model of $[^{18}\text{F}]\text{FMISO}$ PET was the 3-compartment model. The pharmacokinetic model of $[^{18}\text{F}]\text{DiFA}$ is considered the same as for $[^{18}\text{F}]\text{FMISO}$. In these tracers, although the injected activity of the $[^{18}\text{F}]\text{DiFA}$ was almost double that of $[^{18}\text{F}]\text{FMISO}$, the lesion-to-background ratio did not change with increased activity (Additional file 3). $[^{18}\text{F}]\text{DiFA}$ has the advantage of early scan time for reducing patients waiting time, easy synthesis for robust results, and good reproducibility for the assessment of hypoxia status in multi-center trials. In the present investigation, the SUVmax values obtained with $[^{18}\text{F}]\text{DiFA}$ were lower than those

obtained with $[^{18}\text{F}]\text{FMISO}$, in agreement with a preclinical study by Yasui et al. [20].

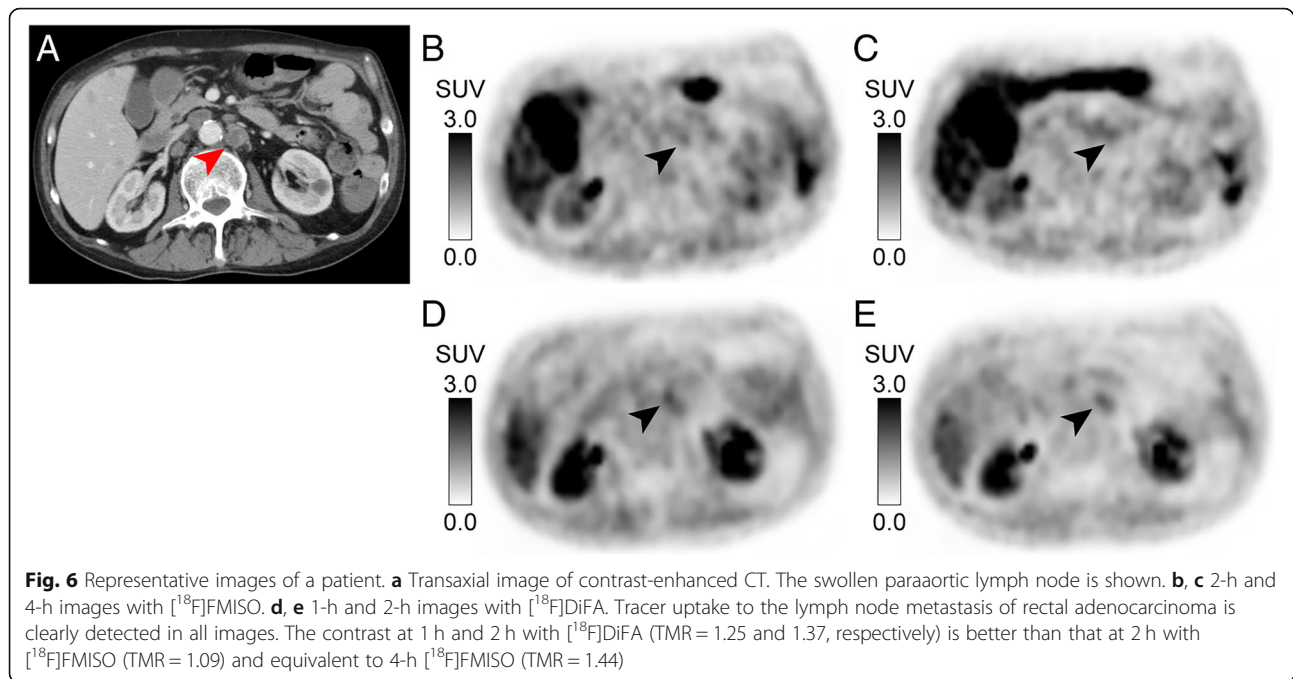
The most important limitation of $[^{18}\text{F}]\text{FMISO}$ is its high lipophilicity, which causes slow tracer accumulation, slow plasma clearance, and low tumor-to-background contrast [2]. Our group showed that $[^{18}\text{F}]\text{FMISO}$ PET for hypoxia imaging achieved better quality at 4 h compared to 2 h, with a better lesion-to-background ratio [21], better differential diagnoses between glioblastoma and lower-grade gliomas at 4 h [22] than at 2 h [23], and high test-retest reproducibility of the tracer distribution at 4 h [17]. In this study, thus, we set the 4-h after injection of $[^{18}\text{F}]\text{FMISO}$ as the gold standard.

New-generation hypoxia tracers have been developed to improve hydrophilicity and accelerate the tracers' clearance from normal oxygenated tissues [24]. A previous report using a single murine xenograft tumor model condition showed $[^{18}\text{F}]\text{FMISO}$, $[^{18}\text{F}]\text{FAZA}$, and $[^{18}\text{F}]\text{HX4}$ demonstrated similar tumor distributions, and highest TBRs for $[^{18}\text{F}]\text{FAZA}$ and $[^{18}\text{F}]\text{HX4}$ were obtained at 2 h p.i. and 3 h p.i., respectively. $[^{18}\text{F}]\text{FMISO}$ and $[^{18}\text{F}]\text{DiFA}$ did not show plateau formation and had better TBR at later time points [24, 25]. There is no clinical study which compared the uptake between $[^{18}\text{F}]\text{FAZA}$ and $[^{18}\text{F}]\text{FMISO}$, while $[^{18}\text{F}]\text{HX4}$ imaging in head and neck cancer patients at 1.5 h p.i. was found to have TMR properties similar to those of $[^{18}\text{F}]\text{FMISO}$ at 2 h p.i. Wei et al. reported that $[^{18}\text{F}]\text{FMISO}$ showed significantly higher uptake than $[^{18}\text{F}]\text{FETNIM}$ in tumor/non-tumor ratio in lung cancer [26]. More data have been accumulated for $[^{18}\text{F}]\text{FAZA}$ than for any other second-generation hypoxia tracers, but the reproducibility of the scans using $[^{18}\text{F}]\text{FAZA}$ has not been established. While a preclinical micro-PET analysis showed voxel-to-voxel reproducibility between two baseline scans performed 24 h apart, another preclinical report in an animal tumor model showed that $[^{18}\text{F}]\text{FAZA}$ uptake was less reproducible after 48 h, even without additional anticancer treatment [5]. There has been no report about the reproducibility of $[^{18}\text{F}]\text{FAZA}$ in a clinical trial. In our preclinical research using ex vivo autoradiography, the uptake of $[^{18}\text{F}]\text{DiFA}$, formerly called HIC101, was shown to have a significant positive correlation with regions of pimonidazole distribution, indicating that $[^{18}\text{F}]\text{DiFA}$ was selectively accumulated in tumor hypoxic regions [20, 27]. Yasui et al. reported

Table 7 Diagnostic accuracy of $[^{18}\text{F}]\text{DiFA}$ PET/CT for the detection of tumor hypoxia

Observer	$[^{18}\text{F}]\text{DiFA}$ 1 h				$[^{18}\text{F}]\text{DiFA}$ 2 h			
	Sensitivity	Specificity	Accuracy	p value*	Sensitivity	Specificity	Accuracy	p value*
No. 1	1.00	0.90	0.95	0.32	1.00	0.70	0.84	0.08
No. 2	0.89	0.70	0.79	0.32	1.00	0.70	0.84	0.08

*McNemar's test



that the tumor-to-muscle ratios were significantly higher as early as at 1 h post-injection. In the current study, the images of 1 h p.i. of $[^{18}\text{F}]$ DiFA and the images of 4 h p.i. of $[^{18}\text{F}]$ FMISO were equivalent, indicating the potential to obtain an image with good contrast at 1 h after injection.

Masaki et al. [28] and Shimizu et al. [7] described the mechanisms of $[^{18}\text{F}]$ FMISO and $[^{18}\text{F}]$ DiFA. In brief, the glutathione-conjugated reductive metabolites of the tracer are present in the hypoxic regions of tumor tissues, suggesting that the tracer undergoes the glutathione conjugation reaction following reductive metabolism in hypoxic cells. The glutathione conjugate of reduced tracer was the major metabolite involved in the hypoxia-specific accumulation. In our preclinical study, while $[^{18}\text{F}]$ DiFA accumulated in hypoxic cells was higher than that of $[^{18}\text{F}]$ FMISO, $[^{18}\text{F}]$ DiFA was rapidly cleared from the blood [7]. When administered to mice, the tumor-to-blood and the tumor-to-muscle ratios of $[^{18}\text{F}]$ DiFA were higher than those of $[^{18}\text{F}]$ FMISO. The rapid clearance may have contributed to the reduced non-specific accumulation of $[^{18}\text{F}]$ DiFA in the background tissues. Therefore, the distribution of $[^{18}\text{F}]$ DiFA may be equally or highly specific to the hypoxic region of tumor tissues compared to that of $[^{18}\text{F}]$ FMISO [7]. In the current human study, the background of $[^{18}\text{F}]$ DiFA tended to be lower compared to that of $[^{18}\text{F}]$ FMISO (Additional file 4: Figure S1). Thus, $[^{18}\text{F}]$ DiFA achieved better contrast imaging of tumor hypoxia with a shorter waiting time compared to $[^{18}\text{F}]$ FMISO via the same mechanism.

The major limitations of this preliminary study were that only seven patients were enrolled for the diagnostic

assessment of hypoxia detection by $[^{18}\text{F}]$ FMISO and $[^{18}\text{F}]$ DiFA and the primary tumors or metastases were varied, rather than restricted to a specific type of lesion. We plan to conduct verification studies on specific carcinomas soon. Since $[^{18}\text{F}]$ DiFA undergoes the same metabolic pathway of $[^{18}\text{F}]$ FMISO in hypoxic cells, the distribution of $[^{18}\text{F}]$ DiFA in tumor tissues might be affected by factors related to glutathione conjugation. Previously, our group investigated the mechanisms of the $[^{18}\text{F}]$ FMISO uptake in three cell lines (FaDu, LOVO, and T24) and found that $[^{18}\text{F}]$ FMISO accumulation was associated with glutathione conjugation ability as well as hypoxic conditions [29]. Similarly, $[^{18}\text{F}]$ DiFA accumulation might be affected by cellular factors such as the cellular reduced glutathione level and glutathione S-transferases, which catalyze glutathione conjugation reactions, and the multidrug resistant protein 1, which exports various kinds of glutathione conjugates out of cells. Therefore, further preclinical and clinical studies are needed to clarify whether these factors actually influence the imaging of $[^{18}\text{F}]$ DiFA. In addition, we studied whether $[^{18}\text{F}]$ FMISO and $[^{18}\text{F}]$ DiFA exhibit the same distribution 48 h apart, but we did not compare $[^{18}\text{F}]$ DiFA and new hypoxia tracers such as $[^{18}\text{F}]$ FAZA or $[^{18}\text{F}]$ HX4. Further research on the reproducibility of $[^{18}\text{F}]$ DiFA findings is also necessary.

Conclusions

The current study revealed 2 important findings. First, $[^{18}\text{F}]$ DiFA is well tolerated and its radiation dose is comparable to that of $[^{18}\text{F}]$ FMISO and other hypoxia tracers. $[^{18}\text{F}]$ DiFA showed very rapid clearance and a large

fraction of renal excretion. Second, [^{18}F]DiFA achieved an equivalent image quality compared with [^{18}F]FMISO, with smaller inter-observer variability. Thus, [^{18}F]DiFA PET enables hypoxia imaging with equivalent contrast in shorter waiting time and would be potentially suitable for a multicenter trial.

Additional files

Additional file 1: Table S1. Reaction sequence for [^{18}F]DiFA radiosynthesis. (DOCX 15 kb)

Additional file 2: The results of laboratory tests. (XLSX 33 kb)

Additional file 3: The lesion-to-background ratio formula. (DOCX 30 kb)

Additional file 4: Figure S1. [^{18}F]DiFA vs. [^{18}F]FMISO (PDF 736 kb)

Abbreviations

[^{18}F]DiFA: 1-(2,2-dihydroxymethyl-3- ^{18}F -fluoropropyl)-2-nitroimidazole; [^{18}F]FAZA: [^{18}F]Fluoroazomycin-arabinofuranoside; [^{18}F]FETNIM: [^{18}F]Fluoroerythronitromidazole; [^{18}F]FMISO: [^{18}F]Fluoromisonidazole; [^{18}F]HX4: [^{18}F]-3-Fluoro-2-(4-((2-nitro-1H-imidazo-1-yl)methyl)-1H-1,2,3-triazol-1-yl)propan-1-ol; CT: Computed tomography; FOV: Field of view; IA: Injected activity; MIP: Maximum intensity projection; MIRD: Medical internal radiation dose; OLINDA/EXM: Organ level internal dose assessment/exponential modeling; OSEM: Ordered-subsets expectation maximization; PET: Positron emission tomography

Acknowledgements

We thank all the staff of the Department of Nuclear Medicine in Hokkaido University Graduate School of Medicine and the Department of Pharmacy, Radiation Section, and the Clinical Research and Medical Innovation Center, and 5-2 ward of Hokkaido University Hospital.

Authors' contributions

SW is the main author, recruited the normal volunteers and patients, and collected and analyzed the data. HM, YK, and KN developed the [^{18}F]DiFA. TS, SO, and NT designed the study. KM acquired and reconstructed the PET data. KI, JK, HY, and KH synthesized and checked the quality of [^{18}F]DiFA and [^{18}F]FMISO. TT and KH recruited the normal volunteers and analyzed the data. All authors have read and approved the final manuscript.

Funding

This work was supported by the Japan Agency for Medical Research and Development (AMED) and the Japan Society for the Promotion of Science (JSPS) KAKENHI Grant # 17 K10428 Ministry of Education, Culture, Sports, Science, and Technology.

Availability of data and materials

The datasets used and/or analyzed during the current study are available from the corresponding author on reasonable request.

Ethics approval and consent to participate

All procedures performed in studies involving human participants were in accordance with the ethical standards of the institutional research committee and with the 1964 Helsinki declaration and its later amendments or comparable ethical standards. The Ethics Committee of Hokkaido University Hospital approved this study (#015-0372 and #017-0154 for healthy volunteer and patient studies, respectively), and written informed consent was obtained from each subject.

Consent for publication

Not applicable

Competing interests

HM is an employee of Nihon Medi-Physics Co., Ltd. The other authors declare that they have no competing interests.

Author details

¹Department of Nuclear Medicine, Graduate School of Medicine, Hokkaido University, Kita-15, Nishi-7, Kita-ku, Sapporo 060-8638, Japan. ²Division of Medical Imaging and Technology, Hokkaido University Hospital, Kita-14, Nishi-5, Kita-ku, Sapporo 060-8648, Japan. ³Department of Radiology, Obihiro Kosei Hospital, West 14 South 10-1, Obihiro 080-0024, Japan. ⁴Central Institute of Isotope Science, Hokkaido University, Kita-15, Nishi-7, Kita-ku, Sapporo 060-8638, Japan. ⁵Department of Pharmacy, Hokkaido University Hospital, Kita-14, Nishi-5, Kita-ku, Sapporo 060-8648, Japan. ⁶Advanced Clinical Research Center, Fukushima Global Medical Science Center, Fukushima Medical University, 1 Hikariga-oka, Fukushima 960-1295, Japan. ⁷Faculty of Pharmaceutical Sciences, Kita-14, Nishi-5, Kita-ku, Sapporo 060-8648, Japan. ⁸Research Centre, Nihon Medi-Physics Co., Ltd., 3-1 Kitasode, Sodegaura 299-0266, Japan. ⁹Department of Radiology, Kyoto Prefectural University of Medicine, Kajii-cho, Kawaramachi-Hirokoji, Kamigyo-ku, Kyoto 602-8566, Japan.

Received: 4 March 2019 Accepted: 5 June 2019

Published online: 05 July 2019

References

- Tamaki N, Hirata K. Tumor hypoxia: a new PET imaging biomarker in clinical oncology. *Int J Clin Oncol*. 2016;21:619–25.
- Koh WJ, Rasey JS, Evans ML, Grierson JR, Lewellen TK, Graham MM, et al. Imaging of hypoxia in human tumors with [^{18}F]fluoromisonidazole. *Int J Radiat Oncol Biol Phys*. 1992;22:199–212.
- Grunbaum Z, Freauff SJ, Ka K, Wilbur DS, Magee S, Rasey JS. Synthesis and characterization of congeners of misonidazole for imaging hypoxia. *J Nucl Med*. 1987;28:68–75.
- Carlin S, Humm JL. PET of hypoxia: current and future perspectives. *J Nucl Med*. 2012;53:1171–4.
- Peeters SGJA, Zegers CML, Lieuwe NG, van Elmpt W, Eriksson J, van Dongen GAMS, et al. A comparative study of the hypoxia PET tracers [(1)(8)F]HX4, [(1)(8)F]FAZA, and [(1)(8)F]FMISO in a preclinical tumor model. *Int J Radiat Oncol Biol Phys*. 2015;91:351–9.
- Wack LJ, Monnich D, van Elmpt W, Zegers CML, Troost EGC, Zips D, et al. Comparison of [^{18}F]FMISO, [^{18}F]FAZA and [^{18}F]HX4 for PET imaging of hypoxia—a simulation study. *Acta Oncol*. 2015;54:1370–7.
- Shimizu Y, Zhao S, Yasui H, Nishijima K-I, Matsumoto H, Shiga T, et al. A novel PET probe “[^{18}F]DiFA” accumulates in hypoxic region via glutathione conjugation following reductive metabolism. *Mol Imaging Biol*. 2019;21:122–9.
- Oh SJ, Chi DY, Mosdzianowski C, Kim JY, Gil HS, Kang SH, et al. Fully automated synthesis of [^{18}F]fluoromisonidazole using a conventional [^{18}F]FDG module. *Nucl Med Biol*. 2005;32:899–905.
- Tang G, Wang M, Tang X, Gan M, Luo L. Fully automated one-pot synthesis of [^{18}F]fluoromisonidazole. *Nucl Med Biol*. 2005;32:553–8.
- Investigator's Brochure for [^{18}F]FMISO. Cancer Imaging Program Division of Cancer Treatment and Diagnosis National Cancer Institute National Institutes of Health. Release Date: February 2013. Available at: https://www.acrin.org/Portals/0/Protocols/6697/6697_FMISO%20-IB_Edition5_ReleaseDate-February5,%202013.pdf. Accessed 24 Apr 2019.
- Savi A, Incerti E, Fallanca F, Bettinardi V, Rossetti F, Monterisi C, et al. First evaluation of PET-based human biodistribution and dosimetry of 18F-FAZA, a tracer for imaging tumor hypoxia. *J Nucl Med*. 2017;58:1224–9.
- Stabin MG, Sparks RB, Crowe E. OLINDA/EXM: the second-generation personal computer software for internal dose assessment in nuclear medicine. *J Nucl Med*. 2005;46:1023–7.
- Graham MM, Peterson LM, Link JM, Evans ML, Rasey JS, Koh WJ, et al. Fluorine-18-fluoromisonidazole radiation dosimetry in imaging studies. *J Nucl Med*. 1997;38:1631–6.
- Doss M, Zhang JJ, Belanger M-J, Stubbs JB, Hostetler ED, Alpaugh K, et al. Biodistribution and radiation dosimetry of the hypoxia marker 18F-HX4 in monkeys and humans determined by using whole-body PET/CT. *Nucl Med Commun*. 2010;31:1016–24.
- Tolvanen T, Lehtio K, Kulmala J, Oikonen V, Eskola O, Bergman J, et al. 18F-Fluoroerythronitromidazole radiation dosimetry in cancer studies. *J Nucl Med*. 2002;43:1674–80.
- Brown JM, Workman P. Partition coefficient as a guide to the development of radiosensitizers which are less toxic than misonidazole. *Radiat Res*. 1980; 82:171–90.

17. Okamoto S, Shiga T, Yasuda K, Ito YM, Magota K, Kasai K, et al. High reproducibility of tumor hypoxia evaluated by 18F-fluoromisonidazole PET for head and neck cancer. *J Nucl Med*. 2013;54:201–7.
18. Wang W, Georgi J-C, Nehmeh SA, Narayanan M, Paulus T, Bal M, et al. Evaluation of a compartmental model for estimating tumor hypoxia via FMISO dynamic PET imaging. *Phys Med Biol*. 2009;54:3083–99.
19. Thorwarth D, Eschmann SM, Paulsen F, Alber M. A kinetic model for dynamic [18F]-Fmiso PET data to analyse tumour hypoxia. *Phys Med Biol*. 2005;50:2209–24.
20. Yasui H, Zhao S, Higashikawa K, Ukon N, Shimizu Y, Matsumoto H, et al. Preclinical evaluation of [18F]DIFA, a novel PET probe for tumor hypoxia, in comparison with [18F]MISO. *J Nucl Med [Internet]*. 2017;58:1027.
21. Kobayashi K, Hirata K, Yamaguchi S, Kobayashi H, Terasaka S, Manabe O, et al. FMISO PET at 4 hours showed a better lesion-to-background ratio uptake than 2 hours in brain tumors. *J Nucl Med*. 2015;56:373.
22. Hirata K, Terasaka S, Shiga T, Hattori N, Magota K, Kobayashi H, et al. (1)(8)F-Fluoromisonidazole positron emission tomography may differentiate glioblastoma multiforme from less malignant gliomas. *Eur J Nucl Med Mol Imaging*. 2012;39:760–70.
23. Yamamoto Y, Maeda Y, Kawai N, Kudomi N, Aga F, Ono Y, et al. Hypoxia assessed by 18F-fluoromisonidazole positron emission tomography in newly diagnosed gliomas. *Nucl Med Commun*. 2012;33:621–5.
24. Lopci E, Grassi I, Chiti A, Nanni C, Cicoria G, Toschi L, et al. PET radiopharmaceuticals for imaging of tumor hypoxia: a review of the evidence. *Am J Nucl Med Mol Imaging*. 2014;4:365–84.
25. Nakata N, Kiriu M, Okumura Y, Zhao S, Nishijima K-I, Shiga T, et al. Comparative evaluation of [(18)F]DIFA and its analogs as novel hypoxia positron emission tomography and [(18)F]FMISO as the standard. *Nucl Med Biol*. 2019;70:39–45.
26. Wei Y, Zhao W, Huang Y, Yu Q, Zhu S, Wang S, et al. A comparative study of noninvasive hypoxia imaging with 18F-fluoroerythronitroimidazole and 18F-fluoromisonidazole PET/CT in patients with lung cancer. *PLoS One*. 2016;11:e0157606.
27. Nakata N, Okumura Y, Nagata E, Kiriu M, Hayashi A, Nishijima K, et al. Evaluation of a new PET hypoxia tracer, [18F]HIC101, in comparison with [18F]FMISO. *J Nucl Med*. 2012;53:1523.
28. Masaki Y, Shimizu Y, Yoshioka T, Tanaka Y, Nishijima K-I, Zhao S, et al. The accumulation mechanism of the hypoxia imaging probe “FMISO” by imaging mass spectrometry: possible involvement of low-molecular metabolites. *Sci Rep*. 2015;5:16802.
29. Masaki Y, Shimizu Y, Yoshioka T, Nishijima K-I, Zhao S, Higashino K, et al. FMISO accumulation in tumor is dependent on glutathione conjugation capacity in addition to hypoxic state. *Ann Nucl Med*. 2017;31:596–604.

Publisher's Note

Springer Nature remains neutral with regard to jurisdictional claims in published maps and institutional affiliations.

Submit your manuscript to a SpringerOpen[®] journal and benefit from:

- Convenient online submission
- Rigorous peer review
- Open access: articles freely available online
- High visibility within the field
- Retaining the copyright to your article

Submit your next manuscript at ► [springeropen.com](https://www.springeropen.com)
